Published in final edited form as:

J Cell Physiol. 2019 November ; 234(11): 20675–20684. doi:10.1002/jcp.28672.

Apical cell protrusions cause vertical deformation of the soft cancer nucleus

Ian A. Kent[a], **Qiao Zhang**[a], **Aditya Katiyar**[b], **Yuan Li**[a], **Shreya Pathak**[a], **Richard B. Dickinson**[a], **Tanmay P. Lele**[a,*]

[a]Department of Chemical Engineering, University of Florida, Gainesville, FL 32611

[b]Department of Mechanical and Aerospace Engineering, University of Florida, Gainesville, FL 32611

Abstract

Breast cancer nuclei have highly irregular shapes, which are diagnostic and prognostic markers of breast cancer progression. The mechanisms by which irregular cancer nuclear shapes develop are not well understood. Here we report the existence of vertical, apical cell protrusions in cultured MDA-MB-231 breast cancer cells. Once formed, these protrusions persist over time scales of hours and are associated with vertically upward nuclear deformations. They are absent in normal mammary epithelial cells (MCF-10A cells). Microtubule disruption enriched these protrusions preferentially in MDA-MB-231 cells compared to MCF-10A cells, while inhibition of non-muscle myosin II (NMMII) abolished this enrichment. Dynamic confocal imaging of the vertical cell and nuclear shape revealed that the apical cell protrusions form first, and in response, the nucleus deforms and/or subsequently gets vertically extruded into the apical protrusion. Over-expression of lamin A/C in MDA-MB-231 cells reduced nuclear deformation in apical protrusions. These data highlight the role of mechanical stresses generated by moving boundaries as well as abnormal nuclear mechanics in the development of abnormal nuclear shapes in breast cancer cells.

Keywords

Cancer nucleus; Protrusions; Microtubule; Nuclear shape; Breast cancer; Lamin A/C

Introduction

That the nucleus is irregularly shaped in cancer has been known since the 1860s (Beale, 1860). In breast cancers, nuclear surface abnormalities are graded and correlate with clinical

*Address correspondence to: Tanmay P. Lele (tlele@che.ufl.edu), Department of Chemical Engineering, Bldg. 723, University of Florida, Gainesville, FL 32611, Ph: 352-392-0317.

Author Contributions

I.A.K., Q.Z., A.K., Y.L., designed, performed experiments and interpreted results. S.P. performed experiments and interpreted results. R.B.D., T.P.L. designed experiments and interpreted results. T.P.L. wrote the manuscript with support from I.A.K., Q.Z., A.K., Y.L., and R.B.D.

Competing Interests

The authors declare no competing interests.

Availability of data

The data that support the findings of this study are available from the corresponding author upon request.

aggressiveness and prognosis (Bussolati, Marchio, Gaetano, Lupo, & Sapino, 2008; Elston & Ellis, 1991). Abnormal nuclear morphologies have strong diagnostic and prognostic importance (Bussolati G, 2014; Giardina et al., 1996; Haroske et al., 1996). Diagnostically useful features in breast cancer include nuclear lobulation, grooves, clefts, or folds in the envelope, changes in nuclear size, alterations in chromatin organization (Imbalzano et al., 2013; Zink, Fischer, & Nickerson, 2004) and changes in number or appearance of nucleoli. Although cancer diagnostics depends critically on microscopic evaluation of patient biopsies, the molecular mechanisms for the abnormal nuclear shapes in cancer are not fully understood (Denais & Lammerding, 2014).

Abnormalities in nuclear morphologies may occur in part due to modifications of higher order chromatin structure and associated alterations in gene expression that are present during breast cancer progression (Barutcu et al., 2016; Fritz et al., 2018). Consistent with this notion, increasing the amount of euchromatin or decreasing heterochromatin through modification of histone modification states mechanically softens the nucleus and causes nuclear blebbing (Stephens, Liu, et al., 2017). Similarly, knockdown of the chromatin remodeling enzymatic subunit BRG1 in breast epithelial cells induces nuclear lobulations and invaginations (Imbalzano et al., 2013). In addition to chromatin alterations, loss of nuclear lamins, a common occurrence in breast cancer, can also induce abnormal nuclear morphologies (Capo-chichi et al., 2011).

The nucleus in cells is constantly acted upon by mechanical stresses (Lele, Dickinson, & Gundersen, 2018). One potential source of mechanical stresses on the nuclear surface is the motion of cell boundaries proximal to the nuclear surface, which produce local deformations in the cell nucleus (Alam et al., 2015; Li et al., 2015). We have shown previously that the process of cell spreading amplifies nuclear shape abnormalities in MDA-MB-231 breast cancer cells, but not in non-malignant human mammary epithelial cells (MCF-10A) (Tocco et al., 2018). These findings suggest the hypothesis that cell protrusions may contribute, at least in part, to local abnormal nuclear deformations in breast cancer cells. In this paper, we report the existence of vertical, apical cell protrusions in cultured MDA-MB-231 breast cancer cells which are absent in MCF-10A cells. These protrusions were associated with vertically upward nuclear deformations. Dynamic imaging of cell spreading confirmed that nuclear deformations develop as a result of dynamic cell protrusion. Taken together, these results highlight the importance of cell-generated mechanical stresses in the development of abnormal nuclear shapes in breast cancer.

Results

Using confocal microscopy, we imaged vertical nuclear shapes in MDA-MB-231 cells (referred to henceforth as MB-231 cells) which are a triple-negative breast cancer cell line with a mesenchymal-like phenotype (Charafe-Jauffret et al., 2006; Chavez, Garimella, & Lipkowitz, 2010; Lacroix & Leclercq, 2004). In two-dimensional culture, single non-malignant mammary epithelial MCF-10A cells which are considered to have a near-normal phenotype (Imbalzano, Tatarkova, Imbalzano, & Nickerson, 2009; Merlo, Basolo, Fiore, Duboc, & Hynes, 1995; Miller et al., 1993; Soule et al., 1990) exhibited a typical vertical shape (x-z profile) with the cell being tallest over the nucleus and becoming gradually flatter

farther away from the nucleus (Figure 1) consistent with our previous observations (Li et al., 2015; Lovett, Shekhar, Nickerson, Roux, & Lele, 2013; Neelam, Hayes, Zhang, Dickinson, & Lele, 2016)). The nucleus resembled a flattened ellipsoid in these cells. While around 90% of MB-231 cells exhibited a similar x-z profile, in the rest of the MB-231 cells, a cell membrane protrusion was present at the apical surface (hereafter called apical cell protrusion, Figure 1). In all MB-231 cells with apical protrusions, the apical surface of the nucleus was deformed into the apical cell protrusion. The deformed nuclei displayed a negative curvature near the opening to the apical cell protrusion mimicking the negative curvature in the cell protrusion (marked by white arrows in Figure 1). Notably, in the x-y plane, cells with such apical protrusions were well-spread, which gave a ‘Mexican-hat’ type appearance to cells in the x-z plane.

To determine why apical cell protrusions form in MB-231 cells, we treated cells with cytoskeletal inhibitors. Upon one hour of treatment with 5 μM nocodazole to depolymerize the microtubule network, apical cell protrusions were substantially enriched in MB-231 cells, occurring in over 50% of the treated cells compared to only about 10% in untreated cells (Figure 2A and Table 1). Apical cell protrusions were also enriched in MCF-10A cells upon nocodazole treatment but to a much smaller extent (Figure 2A and Table 1). In both MB-231 cells and MCF-10A cells, apical cell protrusions were associated with a vertically upward nuclear deformation (Figure 2B and C) in about 60% of cells with apical protrusions.

We have previously shown that vertical nuclear flattening correlates inversely with cell spreading area in fibroblasts (Li et al., 2015), with rounded cells displaying rounded vertical nuclear shapes. Therefore, one possibility is that the presence of apical cell protrusions in a fraction of the MB-231 cell population is due to cells which have not reached a steady state in the cell spreading process after mitosis. Further, nocodazole treatment might result in cell rounding, thereby creating apical cell protrusions and hence deformation of the apical nuclear surface. We therefore compared the degree of cell spreading between control and nocodazole treated cells (Figure S1). While nocodazole treatment severely rounded up some MB-231 cells in culture, we could observe several well-spread cells which had apical cell protrusions and associated nuclear deformation (an example of a confocal series of images is shown in Figure 2D). There was no statistically significant difference between the area of cell spreading between control and nocodazole treated MB-231 cells which displayed apical protrusions. This result argues against the hypothesis that enrichment of apical cell protrusions and vertical nuclear deformation in nocodazole treated cells necessarily requires cell rounding. As trypsinization of cells can also cause rounding of the vertical nuclear cross-section (Li et al., 2015), we further challenged the above hypothesis by causing partial rounding of cells through trypsinization for 30 s before fixation. Partial trypsinization of cells did not induce the development of apical cell protrusions in MB-231 cells, nor deformation of the apical nuclear surface. Trypsinization also did not change the frequency of apical cell protrusions in MB-231 cells (Table 1).

Cell protrusions in the x-y plane of the cell proximal to the nuclear surface cause local nuclear deformations in the direction of protrusions (Alam et al., 2015; Tocco et al., 2018). Relaxation of cell protrusions causes a relaxation of nuclear deformations. To test if vertical

apical protrusions precede vertical nuclear deformation, we imaged the dynamic formation of apical cell protrusions and the vertical shape of the NLS-GFP expressing nucleus using confocal fluorescence microscopy. In these experiments, we treated MB-231 cells with nocodazole to enrich apical cell protrusions.

Figure 3A shows the dynamic formation of an apical protrusion upon nocodazole addition at time t = 0 min, and the corresponding x-z nuclear profiles tracked by staining lipid membranes with DiI (a lipophilic tracer used to visualize the cell membrane). The nucleus can be seen to round up vertically with changes to the vertical cellular shape. At around 20 minutes, a small apical protrusion is seen to develop which subsequently becomes large and a major portion of the nucleus is drawn into the protrusion. These results demonstrate that the apical protrusions form first, followed by vertically upward deformation of the nucleus.

We also tracked the F-actin network using RFP-Lifeact during the development of the vertical protrusion (Figure 3B), and observed similar behavior where the vertical shape of the nucleus roughly mimicked the vertical shape of the cell. Extension of the apical surface of the nucleus extended the apical surface while relaxation caused the apical nuclear surface to relax back. No stress fibers were visible in these cells on top of the nucleus. Inward movement of the boundaries in the basal plane and their outward movement in the apical plane correlate with changes in the shape of the nucleus.

Remarkably, the life time of the protrusions was several hours (Figure S2) and they were observed to move across the cell surface in a seemingly random fashion, sometimes changing in size. In response, the apical surface of the nucleus stayed deformed for time scales of hours before collapsing back due to loss of the protrusion (Figure S2).

Microtubule depolymerization is known to increase actomyosin contractility through activation of the GTPase RhoA (Burakov, Nadezhdina, Slepchenko, & Rodionov, 2003; Wittmann & Waterman-Storer, 2001). We hypothesized therefore that the enrichment of apical protrusions in microtubule disrupted cells may be caused by NMMII mediated contraction of the cortical F-actin cytoskeleton. If apical cell protrusions are dependent on NMMII, then this would also explain their enrichment upon nocodazole treatment. F-actin was localized along the periphery of these protrusions while phosphorylated myosin (visualized with a phospho-specific antibody) was found to be present in a diffuse pattern in the protrusion with slight enrichment at parts of the periphery (Figure 4A). Treatment of MB-231 cells with blebbistatin to inhibit myosin activity completely suppressed apical cell protrusions (Figure 4B and Table 1). To determine if the increase in apical protrusions in microtubule disrupted cells was NMMII dependent, we treated MB-231 cells with blebbistatin and nocodazole together. The occurrence of apical cell protrusions was again greatly reduced compared to treatment with nocodazole alone and was similar to the occurrence in untreated cells (Table 1). Collectively, these results suggest that apical cell protrusions are NMMII dependent.

As MB-231 cells have low levels of lamin A/C (Matsumoto et al., 2015) which softens the nucleus (Denais & Lammerding, 2014), we hypothesized that over-expressing lamin A/C in these cells will reduce the apical nuclear protrusions. Over-expression of GFP lamin A/C in

these cells abolished the nuclear deformations associated with apical protrusions, although the occurrence of apical protrusions themselves was increased (Figure 4C and D, Table 1). These results are consistent with the hypothesis that the MB-231 nucleus is deformed upward into the apical protrusion because it is soft due to low levels of lamin A/C(Davidson, Sliz, Isermann, Denais, & Lammerding, 2015; Neelam et al., 2015; Stephens, Banigan, Adam, Goldman, & Marko, 2017).

Discussion

We report the existence of vertically upward protrusions in spread breast cancer cells. These cells resemble a ‘Mexican hat’ in the x-z plane. The protrusions are associated with apical nuclear deformations. The enrichment of apical MB-231 cell protrusions after nocodazole treatment was abrogated upon NMMII inhibition. This suggests that enrichment of protrusions in nocodazole treated cells may be due to the well-known upregulation of NMMII activity due to microtubule depolymerization.

While the mechanism for the generation of apical cell protrusions is not clear, it is possible that NMMII mediated contraction extrudes the apical cell membrane and associated cortex upward. The protrusions are dynamic and seem to change in orientation along the apical cell surface but are persistent over time scales of hours. The corresponding deformations of the apical nuclear surface correlate with the presence (or absence) of protrusions and persist over similarly long times (Figure 4 and Figure S2).

We have previously suggested that motion of boundaries away from or toward the nuclear surface can exert tensile or compressive stresses that pull or push on the nuclear surface (reviewed in (Lele et al., 2018)). The dynamic behaviors of the apical surface of the nucleus in response to the moving apical cell protrusions appear consistent with this model. How the apical protrusions might generate stress on the nucleus is not clear, but we have previously proposed that it is due to frictional transmission of stress between the cell boundary and the nuclear surface, likely through F-actin filaments (Li et al., 2015). Along these lines, disruption of F-actin by treatment with cytochalasin D in MB-231 cells caused severe cell rounding and a long, almost cylindrical vertically upward shape of the cell, but the vertical nuclear shape did not appear correspondingly severely deformed (Figure S3). This at least seems consistent with a role for F-actin in transmitting stress to the nuclear surface in MB-231 cells. In untreated MB-231 cells, apical protrusions were always associated with a nuclear protrusion, but 40% of apical cell protrusions in nocodazole treated cells were not associated with vertical nuclear deformations (Figure 2B). As nocodazole treatment altered F-actin filament organization (Figure S4), it is possible that depletion of F-actin filaments in nocodazole treated cells reduces stress transmission from the protruding boundary to the nuclear surface, and reduces upward deformation of the nucleus in response to apical protrusions.

Cancer cells frequently have low levels of the nuclear lamins, which can also contribute to irregular nuclear shapes (Chen et al., 2018; Dahl, Ribeiro, & Lammerding, 2008; Irianto, Pfeifer, Ivanovska, Swift, & Discher, 2016; Lammerding et al., 2006; Uhler & Shivashankar, 2018). Our finding that over-expressing lamin A/C reduced the apical nuclear deformations

in nocodazole treated cells without having an effect on apical cell protrusions, supports the concept that the pliability of the cancer nucleus is an important determinant of its response to cellular mechanical stresses. The extent to which abnormal nuclear shapes can develop in breast cancer independent of cellular stresses is not clear. At least one study has suggested that the abnormal phenotypes generated after BRG1 knockdown may not depend on the cytoskeleton or alterations in lamins (Imbalzano et al., 2013). However, it is experimentally difficult to completely eliminate all cellular stresses on the nuclear surface. We propose here that studies of the mechanism of stress generation on the nuclear surface, and studies of the mechanisms underlying abnormal nuclear response to these mechanical stresses will both be required for a complete understanding of cancer nuclear dysmorphia.

Materials and Methods

Cell Culture and Transfection

MDA-MB-231 cells (ATCC HTB-26) were cultured in an incubator maintained at 37°C with 5% CO2 under full growth medium consisting of Dulbecco's Modified Eagle Medium (Gibco) supplemented with 10% Donor Bovine Serum (Gibco), 1% Penicillin-Streptomycin (Gibco), 1% Non-Essential Amino Acids (Gibco), and 1% L-glutamine (Gibco). MCF-10A cells were cultured in full growth medium consisting of DMEM/F12 (Gibco) with 5% Donor Horse Serum, 20 ng/mL epidermal growth factor (Corning), 10 μg/mL insulin, 0.5 μg/mL hydrocortisone, 100 ng/mL cholera toxin, and 1% penicillin-streptomycin. Transfections of GFP-Lamin A, GFP-H1.1 or RFP-lifeact (iBidi) were performed with Lipofectamine 3000 (ThermoFisher Scientific) in OptiMEM serum-free media (ThermoFisher) following the manufacturer's suggested protocols. Transduction of Ad-NLS-GFP (a gift from Dr. Daniel Conway, originally from Vector Biosystems INC.) were performed with polybrene at final concentration of 5 μg/ml in normal culture medium.

Drug Treatment and Cell Fixation

MDA-MB-231 or MCF-10A cells were cultured on glass-bottom dishes (WPI) coated with 5 μg/mL fibronectin overnight at 4°C. After the cells were allowed to grow for >24 hours, the cell medium was replaced with full growth medium containing 5 μM nocodazole (Sigma-Aldrich), 50 μM blebbistatin (EMD Millipore), both 5 μM nocodazole and 50 μM blebbistatin, 100 nM cytochalasin D, or 0.3% dimethyl sulfoxide (DMSO) as a control. The cells were incubated for one hour in 37°C at 5% CO_2 concentration, after which the cells were fixed by the following steps: simultaneous fixation and extraction by a solution of 0.5% glutaraldehyde, 0.8% fomaldehyde, and 0.5% Triton X-100 in PBS, fixation for a further 10 minutes by 1% formaldehyde in PBS, incubation for 10 minutes with freshly prepared 1% (w/v) sodium borohydride ($NaBH_4$, Fisher Scientific) in PBS, and blocking with 1% bovine serum albumin (BSA) in PBS for 30 minutes. The cells were rinsed with sterile PBS in between each step, and all steps were performed at room temperature. To stain for microtubules, cells were incubated with 2 μg/mL polyclonal anti-alpha-tubulin from rabbit (Abcam) in 1% BSA for one hour, followed by incubation with an Alexa Fluor 594 goat anti-rabbit secondary antibody at 4 μg/mL for one hour, also in 1% BSA. F-actin and the nucleus were stained simultaneously by room temperature incubation of the cells with

phalloidin-Alexa Fluor 488 (Life Technologies) at a dilution of 1:40 and Hoechst 33342 (Life Technologies) at 1:200 dilution in 1% BSA in PBS.

Partial Trypsinization and Fixation

Cells were partially trypsinized to round the cells in the absence of an agent depolymerizing microtubules. Cell culture medium was removed, and the cells were rinsed once with 37°C PBS. The PBS was removed and 0.25% trypsin (Corning) at 37°C was added for 30 seconds, at which point 37°C full growth cell medium was added to the dish to inactivate the trypsin. All liquid was then removed from the dish, and the samples were fixed with 4% formaldehyde for 15 minutes. The samples were blocked in 1% BSA and stained with Hoechst 33342 and phalloidin-Alexa Fluor 488, diluted 1:200 and 1:40 respectively, in PBS with 1% BSA.

Apical Protrusion Analysis and Statistical Analysis

Image stacks of fixed cells were visually analyzed in FIJI, a distribution of ImageJ (NIH). Cells were categorized by whether an apical protrusion as defined in the Results section was visible in a profile view. Cells in which the entire nucleus was in a protruding part were not considered as having apical protrusions and were not counted as such.

Live cell Imaging

MDA-MB-231 cells were seeded on glass-bottom dishes and transfected with GFP-histone H1.1 and/or RFP-Lifeact to visualize the nucleus and F-actin, respectively. In some experiments, MDA-MB-231 cells were transduced with Ad-NLS-GFP to visualize the nucleus. Invitrogen™ Fast DiI™ (D-7756) lipophilic tracer was used to visualize the cell membrane. The transfected cells were allowed to spread for >24 hours. The cells were imaged on a Nikon TE2000/Ti2 microscope with a Nikon A1 confocal unit using a 60× oil immersion objective. The confocal images were collected at 1 micron step-size in the z-direction. The Z-stacks were used to reconstruct x-y or x-z cross-sections to visualize the dynamics using Nikon elements software.

Supplementary Material

Refer to Web version on PubMed Central for supplementary material.

Acknowledgements

R.B.D.’s contribution is based upon work supported by (while serving at) the National Science Foundation.

Funding Sources

This work was supported by award from the National Institutes of Health [R01 EB014869 (T.P.L.)].

References

Alam SG, Lovett D, Kim DI, Roux K, Dickinson RB, & Lele TP (2015). The nucleus is an intracellular propagator of tensile forces in NIH 3T3 fibroblasts. J Cell Sci, 128(10), 1901–1911. doi:10.1242/jcs.161703 [PubMed: 25908852]

Barutcu AR, Hong D, Lajoie BR, McCord RP, van Wijnen AJ, Lian JB, … Stein GS (2016). RUNX1 contributes to higher-order chromatin organization and gene regulation in breast cancer cells. Biochim Biophys Acta, 1859(11), 1389–1397. doi:10.1016/j.bbagrm.2016.08.003 [PubMed: 27514584]

Beale L (1860). Examination of sputum from a case of cancer of the pharynx and the adjacent parts. Archives of Medicine, London, 2(44).

Burakov A, Nadezhdina E, Slepchenko B, & Rodionov V (2003). Centrosome positioning in interphase cells. J Cell Biol, 162(6), 963–969. doi:10.1083/jcb.200305082 [PubMed: 12975343]

Bussolati G, Marchio C, Gaetano L, Lupo R, & Sapino A (2008). Pleomorphism of the nuclear envelope in breast cancer: a new approach to an old problem. J Cell Mol Med, 12(1), 209–218. [PubMed: 18053086]

Bussolati G, M. F, Asioli S, Annaratone L, Sapino, Marchio C (2014). To be or not to be in a good shape": Diagnostic and Clinical Value of Nuclear Shape Irregularities in Thyroid and Breast Cancer In Heras S. a. (Ed.), Advances in Experimental Medicine and Biology: Cancer Biology and the Nuclear Envelope.

Capo-chichi CD, Cai KQ, Smedberg J, Ganjei-Azar P, Godwin AK, & Xu XX (2011). Loss of A-type lamin expression compromises nuclear envelope integrity in breast cancer. Chin J Cancer, 30(6), 415–425. [PubMed: 21627864]

Charafe-Jauffret E, Ginestier C, Monville F, Finetti P, Adélaïde J, Cervera N, … Bertucci F (2006). Gene expression profiling of breast cell lines identifies potential new basal markers. Oncogene, 25(15), 2273–2284. doi:10.1038/sj.onc.1209254 [PubMed: 16288205]

Chavez KJ, Garimella SV, & Lipkowitz S (2010). Triple negative breast cancer cell lines: one tool in the search for better treatment of triple negative breast cancer. Breast Dis, 32(1–2), 35–48. doi: 10.3233/BD-2010-0307A0762P651Q334681[pii] [PubMed: 21778573]

Chen NY, Kim P, Weston TA, Edillo L, Tu Y, Fong LG, & Young SG (2018). Fibroblasts lacking nuclear lamins do not have nuclear blebs or protrusions but nevertheless have frequent nuclear membrane ruptures. Proc Natl Acad Sci U S A, 115(40), 10100–10105. doi:10.1073/pnas. 1812622115 [PubMed: 30224463]

Dahl KN, Ribeiro AJ, & Lammerding J (2008). Nuclear shape, mechanics, and mechanotransduction. Circ Res, 102(11), 1307–1318. [PubMed: 18535268]

Davidson PM, Sliz J, Isermann P, Denais C, & Lammerding J (2015). Design of a microfluidic device to quantify dynamic intra-nuclear deformation during cell migration through confining environments. Integr Biol (Camb), 7(12), 1534–1546. doi:10.1039/c5ib00200a [PubMed: 26549481]

Denais C, & Lammerding J (2014). Nuclear mechanics in cancer. Adv Exp Med Biol, 773, 435–470. doi:10.1007/978-1-4899-8032-8_20 [PubMed: 24563360]

Elston CW, & Ellis IO (1991). Pathological prognostic factors in breast cancer. I. The value of histological grade in breast cancer: experience from a large study with long-term follow-up. Histopathology, 19(5), 403–410. [PubMed: 1757079]

Fritz AJ, Ghule PN, Boyd JR, Tye CE, Page NA, Hong D, … Stein GS (2018). Intranuclear and higher-order chromatin organization of the major histone gene cluster in breast cancer. J Cell Physiol, 233(2), 1278–1290. doi:10.1002/jcp.25996 [PubMed: 28504305]

Giardina C, Renzulli G, Serio G, Caniglia DM, Lettini T, Ferri C, … Delfino VP (1996). Nuclear morphometry in node-negative breast carcinoma. Anal Quant Cytol Histol, 18(5), 374–382. [PubMed: 8908309]

Haroske G, Dimmer V, Friedrich K, Meyer W, Thieme B, Theissig F, & Kunze KD (1996). Nuclear image analysis of immunohistochemically stained cells in breast carcinomas. Histochem Cell Biol, 105(6), 479–485. [PubMed: 8791108]

Imbalzano KM, Cohet N, Wu Q, Underwood JM, Imbalzano AN, & Nickerson JA (2013). Nuclear shape changes are induced by knockdown of the SWI/SNF ATPase BRG1 and are independent of cytoskeletal connections. PLoS One, 8(2), e55628. doi:10.1371/journal.pone.0055628 [PubMed: 23405182]

Imbalzano KM, Tatarkova I, Imbalzano AN, & Nickerson JA (2009). Increasingly transformed MCF-10A cells have a progressively tumor-like phenotype in three-dimensional basement membrane culture. Cancer Cell Int, 9(1), 7. [PubMed: 19291318]

Irianto J, Pfeifer CR, Ivanovska IL, Swift J, & Discher DE (2016). Nuclear lamins in cancer. Cell Mol Bioeng, 9(2), 258–267. doi:10.1007/s12195-016-0437-8 [PubMed: 27570565]

Lacroix M, & Leclercq G (2004). Relevance of breast cancer cell lines as models for breast tumours: an update. Breast Cancer Res Treat, 83(3), 249–289. doi:10.1023/B:BREA.0000014042.54925.cc [PubMed: 14758095]

Lammerding J, Fong LG, Ji JY, Reue K, Stewart CL, Young SG, & Lee RT (2006). Lamins A and C but not lamin B1 regulate nuclear mechanics. J Biol Chem, 281(35), 25768–25780. doi:10.1074/jbc.M513511200 [PubMed: 16825190]

Lele TP, Dickinson RB, & Gundersen GG (2018). Mechanical principles of nuclear shaping and positioning. J Cell Biol, 217(10), 3330–3342. doi:10.1083/jcb.201804052 [PubMed: 30194270]

Li Y, Lovett D, Zhang Q, Neelam S, Kuchibhotla RA, Zhu R, … Dickinson RB (2015). Moving cell boundaries drive nuclear shaping during cell spreading. Biophysical Journal, 109(4), 670–686. doi:10.1016/j.bpj.2015.07.006 [PubMed: 26287620]

Lovett DB, Shekhar N, Nickerson JA, Roux KJ, & Lele TP (2013). Modulation of Nuclear Shape by Substrate Rigidity. Cell Mol Bioeng, 6(2), 230–238. doi:10.1007/s12195-013-0270-2 [PubMed: 23914256]

Matsumoto A, Hieda M, Yokoyama Y, Nishioka Y, Yoshidome K, Tsujimoto M, & Matsuura N (2015). Global loss of a nuclear lamina component, lamin A/C, and LINC complex components SUN1, SUN2, and nesprin-2 in breast cancer. Cancer Med, 4(10), 1547–1557. doi:10.1002/cam4.495 [PubMed: 26175118]

Merlo GR, Basolo F, Fiore L, Duboc L, & Hynes NE (1995). p53-dependent and p53-independent activation of apoptosis in mammary epithelial cells reveals a survival function of EGF and insulin. J Cell Biol, 128(6), 1185–1196. [PubMed: 7896881]

Miller FR, Soule HD, Tait L, Pauley RJ, Wolman SR, Dawson PJ, & Heppner GH (1993). Xenograft model of progressive human proliferative breast disease. J Natl Cancer Inst, 85(21), 1725–1732. [PubMed: 8411256]

Neelam S, Chancellor TJ, Li Y, Nickerson JA, Roux KJ, Dickinson RB, & Lele TP (2015). Direct force probe reveals the mechanics of nuclear homeostasis in the mammalian cell. Proc Natl Acad Sci U S A, 112(18), 5720–5725. doi:10.1073/pnas.1502111112 [PubMed: 25901323]

Neelam S, Hayes PR, Zhang Q, Dickinson RB, & Lele TP (2016). Vertical uniformity of cells and nuclei in epithelial monolayers. Sci Rep, 6, 19689. doi:10.1038/srep19689 [PubMed: 26795751]

Soule HD, Maloney TM, Wolman SR, Peterson WD Jr., Brenz R, McGrath CM, … Brooks SC (1990). Isolation and characterization of a spontaneously immortalized human breast epithelial cell line, MCF-10. Cancer Res, 50(18), 6075–6086. [PubMed: 1975513]

Stephens AD, Banigan EJ, Adam SA, Goldman RD, & Marko JF (2017). Chromatin and lamin A determine two different mechanical response regimes of the cell nucleus. Mol Biol Cell, 28(14), 1984–1996. doi:10.1091/mbc.E16-09-0653 [PubMed: 28057760]

Stephens AD, Liu PZ, Banigan EJ, Almassalha LM, Backman V, Adam SA, … Marko JF (2017). Chromatin histone modifications and rigidity affect nuclear morphology independent of lamins. Mol Biol Cell. doi:10.1091/mbc.E17-06-0410

Tocco VJ, Li Y, Christopher KG, Matthews JH, Aggarwal V, Paschall L, … Lele TP (2018). The nucleus is irreversibly shaped by motion of cell boundaries in cancer and non-cancer cells. J Cell Physiol, 233(2), 1446–1454. doi:10.1002/jcp.26031 [PubMed: 28542912]

Uhler C, & Shivashankar GV (2018). Nuclear Mechanopathology and Cancer Diagnosis. Trends Cancer, 4(4), 320–331. doi:10.1016/j.trecan.2018.02.009 [PubMed: 29606315]

Wittmann T, & Waterman-Storer CM (2001). Cell motility: can Rho GTPases and microtubules point the way? J Cell Sci, 114(Pt 21), 3795–3803. [PubMed: 11719546]

Zink D, Fischer AH, & Nickerson JA (2004). Nuclear structure in cancer cells. Nat Rev Cancer, 4(9), 677–687. [PubMed: 15343274]

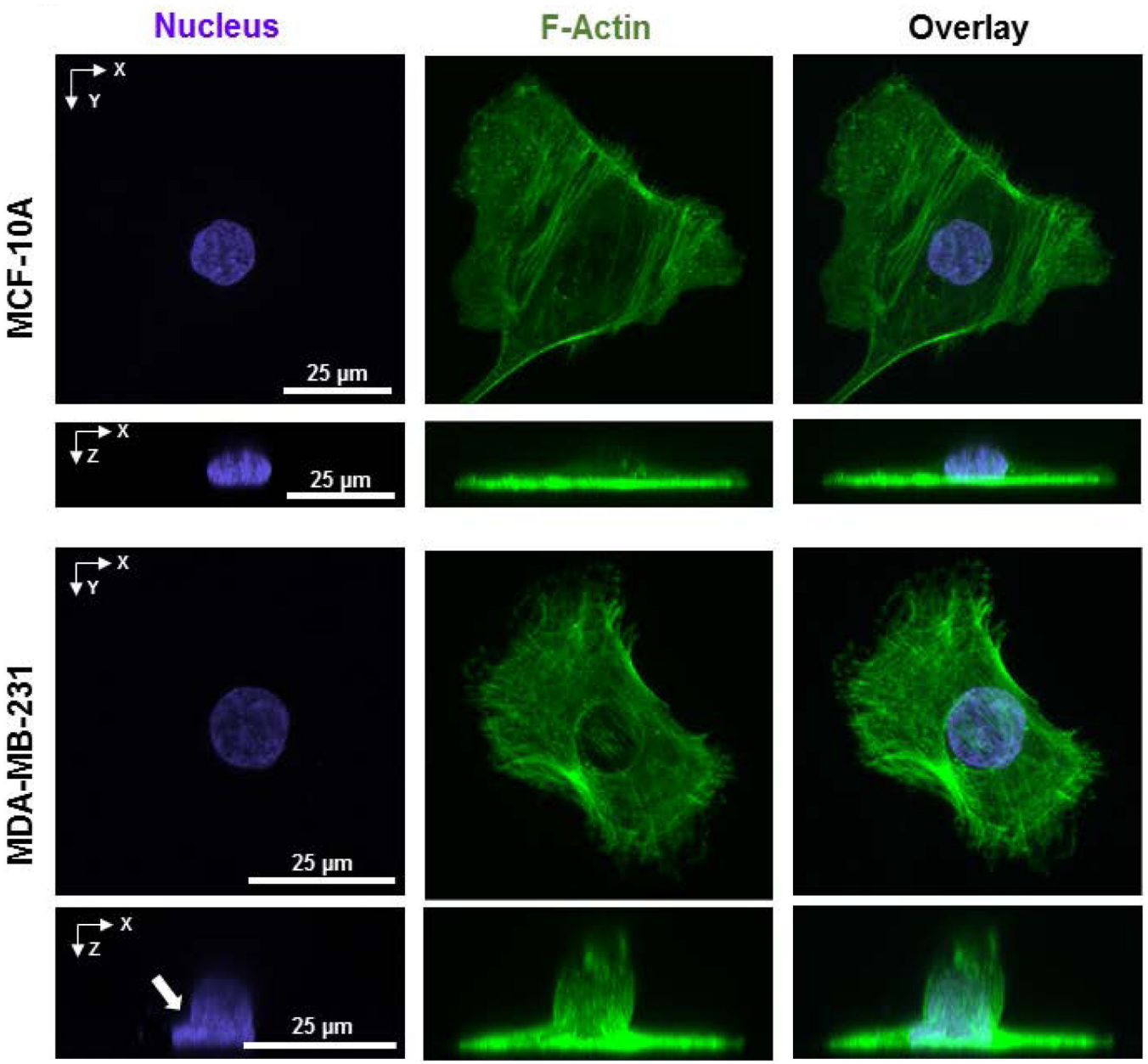

Figure 1.

The presence of apical cell protrusions with associated nuclear deformation in MB-231 cells. Images show representative fluorescent images of x-y and x-z cross-sections of an MCF-10A cell (top) and MB-231 cells (bottom). The MB-231 cell has a ‘Mexican hat’ type appearance due to the local apical cell protrusion in an otherwise well-spread cell.

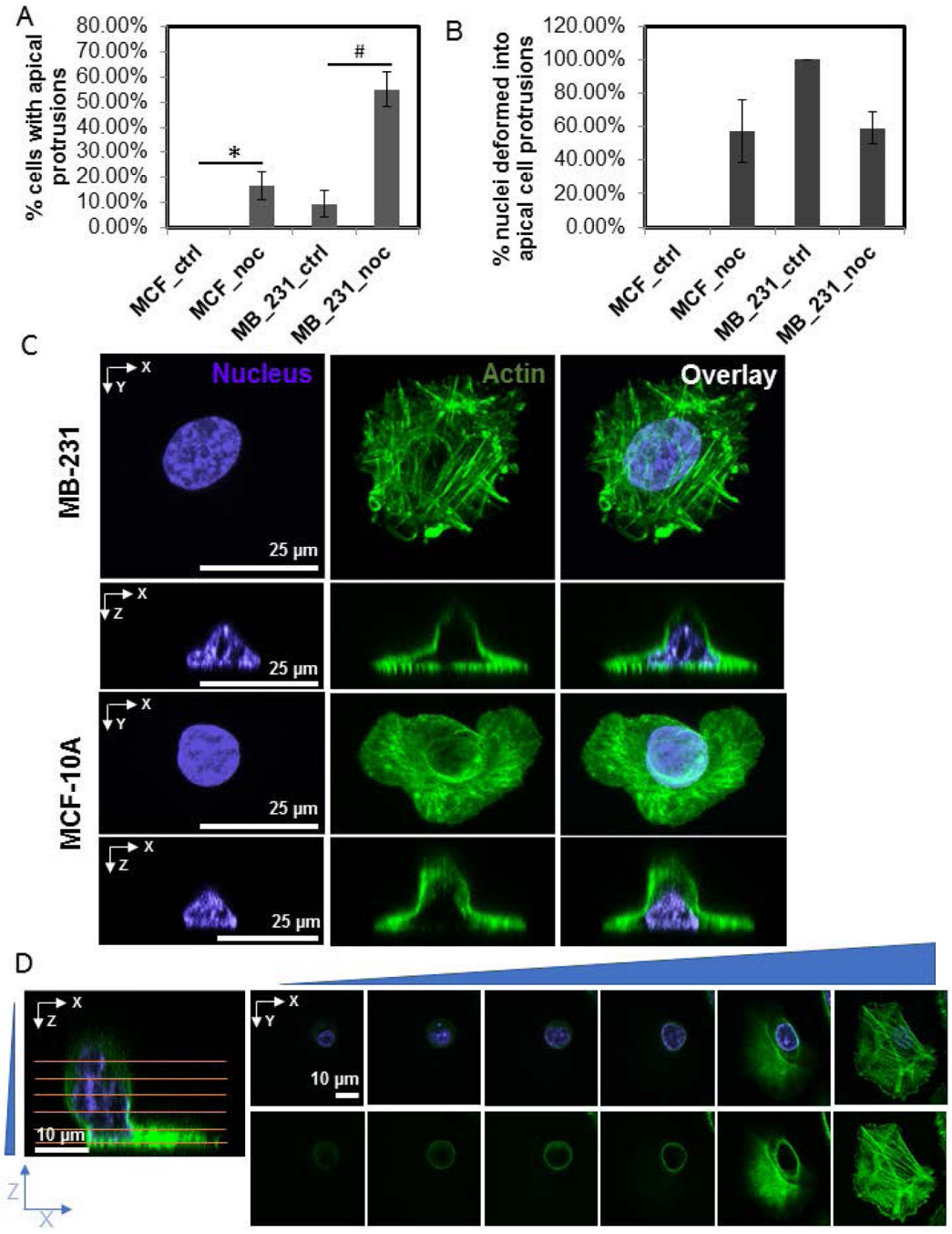

Figure 2.

Nocodazole treatment enriches apical cell protrusions in MB-231 cells. A) Percentage of fixed cells with apical protrusions under various. Chi-square test was used to test statistical differences. *or #, $p<0.05$. $N > 30$ cells for each condition (MCF_ctrl: untreated MCF-10A cells; MB_231_ctrl: untreated MB-231 cells; MCF_noc and MB_231_noc: MCF-10A cells and MB-231 cells respectively treated with 5 µM nocodazole). Error bars indicate SEM. B) Percentage of cells with an apical cell protrusion in which the nuclear shape was vertically deformed into the protrusion. Error bars are SEM. C) Representative fluorescent images of

an MB-231 and MCF-10A cell treated with nocodazole for 1 hr, showing the apical cell protrusion and associated vertical nuclear deformation. D) Fluorescent images show confocal images at different planes (marked by horizontal lines) of an MB-231 cell treated with nocodazole. The apical protrusion is present in an otherwise well-spread cell.

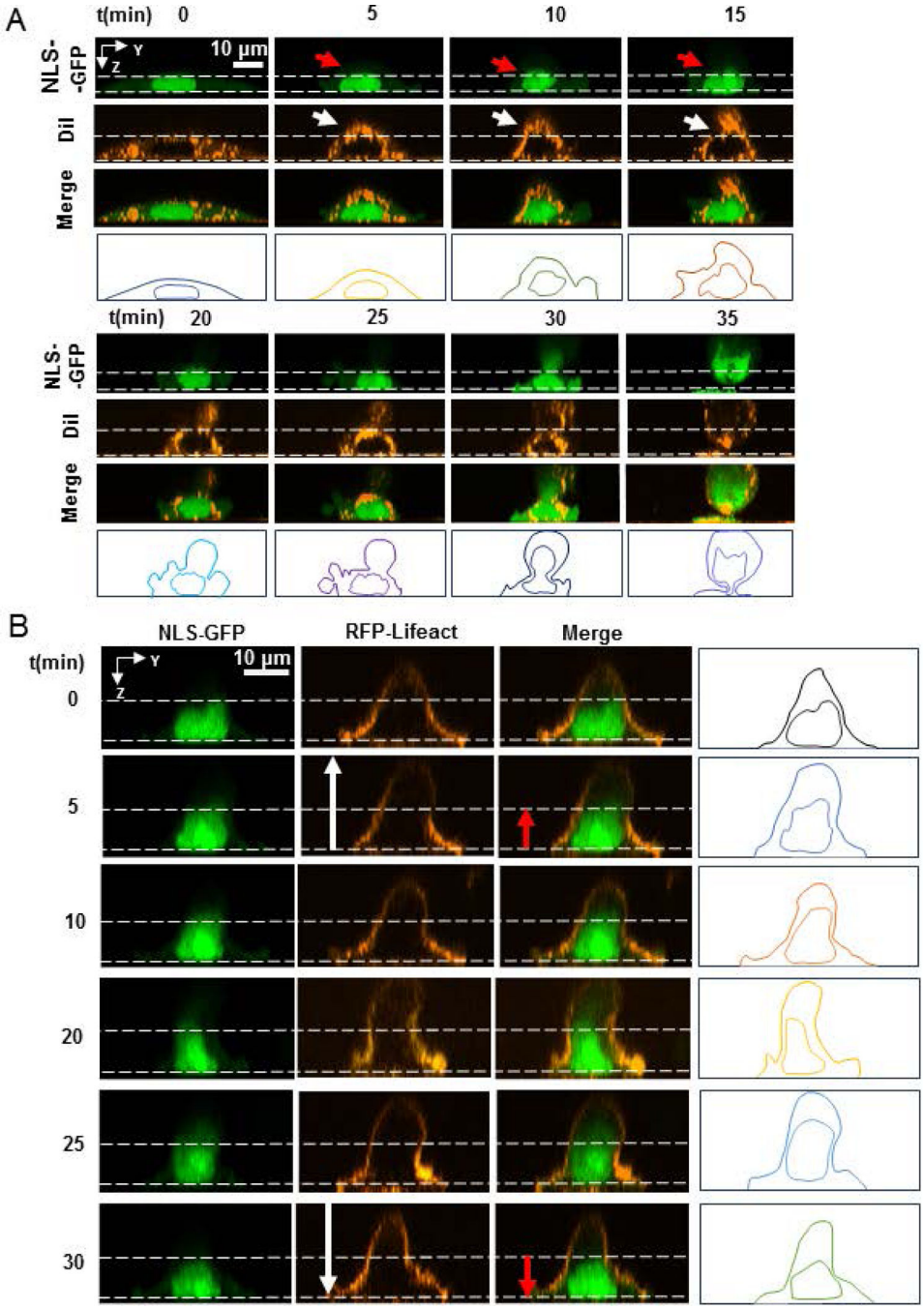

Figure 3.

Apical cells protrusion precedes vertical nuclear deformation. A) Reconstructed fluorescent time-lapse images of the vertical cross-section of a live cell expressing NLS-GFP and treated with lipophilic tracer DiI showing the formation of a vertical protrusion in the cell membrane near the nucleus (white arrows) and the consequent deformation of the nucleus (red arrows) after treatment with 5μM nocodazole at time t = 0 min. For reference, vertical dashed lines indicate the initial position of the nucleus and cell membrane. B) Reconstructed fluorescent time-lapse images of the vertical cross-section of a living cell expressing NLS-

GFP and RFP-LifeAct showing the formation and retraction of a vertical cell protrusion near the nucleus (white arrows) and the consequent deformation of the nucleus (red arrows) after treatment with nocodazole at t = 0 min. Vertical dashed lines indicate the initial position of the nucleus for reference.

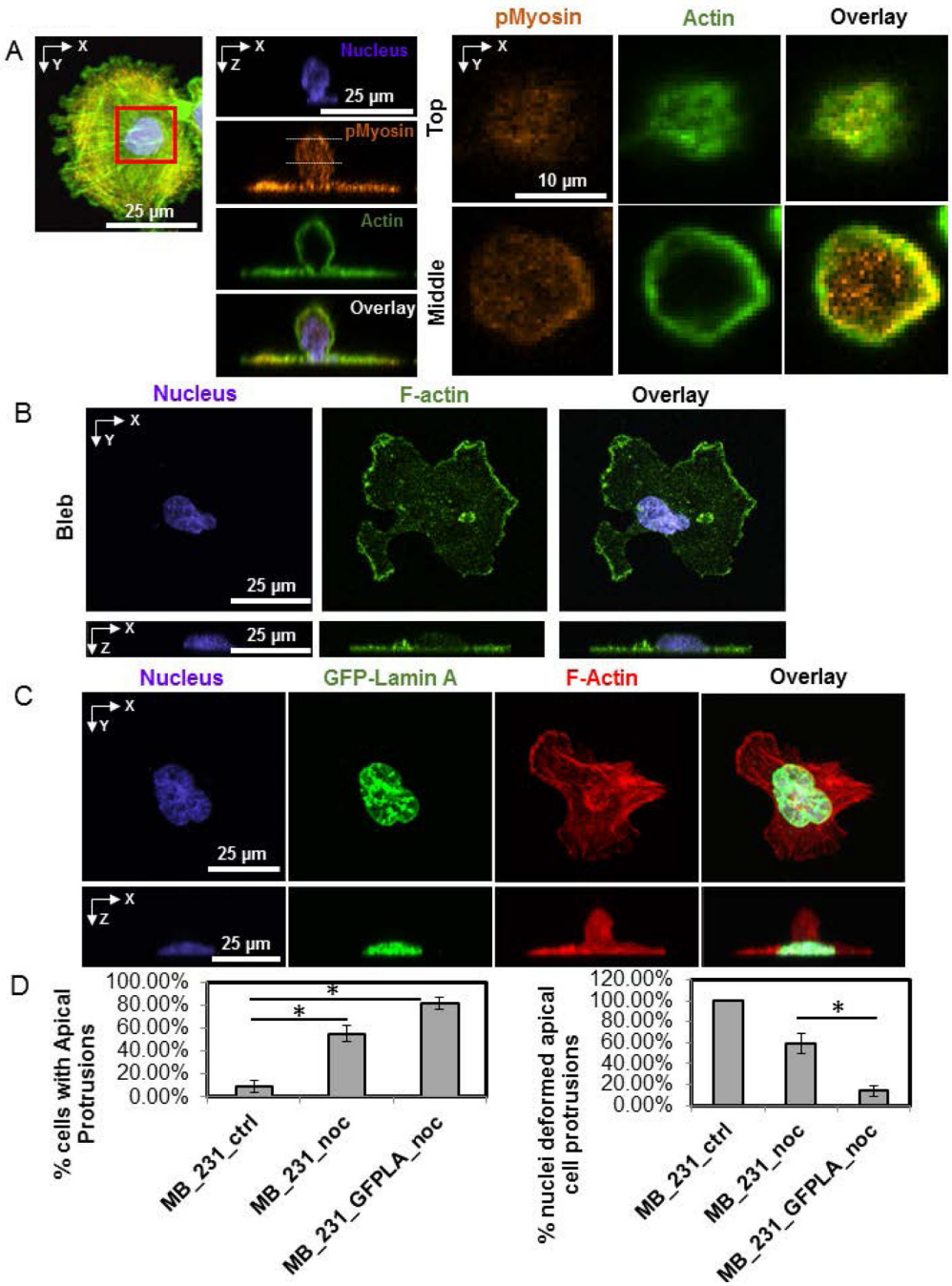

Figure 4.

Apical cell protrusions are NMMII dependent, while vertical nuclear deformation is reduced upon over-expression of GFP-Lamin A. A) An MB-231 cell treated with nocodazole for 1 hr before fixation and stained for pMyosin (orange), F-actin (green) and nucleus (blue). Inset at two z-positions (top and middle planes) shows the distribution of F-actin and pMyosin in the apical cell protrusion. B) Fluorescent images show an example of a MB-231 cell treated with blebbistatin, which abrogated the apical cell protrusion. C) Images show a GFP-Lamin A expressing cell treated with nocodazole for 1 hr before fixation. An apical protrusion is

clearly visible, but with no vertically upward deformation. D) Bar plot shows the frequency of cells with apical protrusions of MDA-MB-231 cells (left) and frequency of nuclei deformed into the apical cell protrusions. (MB_231_ctrl: untreated MB-231 cells; MB_231_noc: MB-231 cells treated with 5 μM nocodazole; MB_231_GFPLA_noc: MB-231 cells expressing GFP-Lamin A and treated with 5 μM nocodazole). Error bar is SEM. At least 32 samples from 3 different dishes are analyzed. Chi-square test with Bonferroni correction was used to test statistical differences. *, $p<0.05$.

Table 1.

Occurrence of apical cell protrusions and associated nuclear shape changes.

Cell and Condition	% cells with apical protrusions
MCF_ctrl	0%
MCF_noc	17% ± 6% *
MB_231_ctrl	9% ± 5%
MB_231_noc	55% ± 7% ##
MB_231_bleb	0%
MB_231_bleb_noc	15% ± 6%
MB_231_tryp 30 sec	11% ± 5%
MB_231_CytoD	17% ± 6%
MB_231_CytoD_noc	39% ± 8% ###
MB_231_GFPLA_noc	81% ± 5% ##

###: $p < 0.001$;

##: $p < 0.01$;

*: $p < 0.05$.

All statistical comparisons (Chi-sq test with Bonferroni correction) are with respect to corresponding control for a given cell type). ctrl: control; noc: nocodazole; bleb: blebbistatin; tryp 30 sec: trypsinization for 30 s; CytoD: cytochalasin D; GFPLA: GFP-Lamin A. N > 30 cells for each condition. Values represent Mean ± SEM.